# Grain Boundary Sliding in the Presence of Grain Boundary Precipitates during Transient Creep

X.-J. WU and A.K. KOUL

A constitutive rate equation for grain boundary sliding (GBS), in the presence of grain boundary precipitates, is developed. Langdon's GBS model is modified by incorporating physically defined back stresses opposing dislocation glide and climb and by modifying the grain size dependence of creep rate. The rate equation accurately predicts the stress dependence of minimum creep rate and change in activation energy occurring as a result of changing the grain boundary precipitate distribution in complex Ni-base superalloys. The rate equation, along with the mathematical formulations for internal stresses, is used to derive a transient creep model, where the transient is regarded as the combination of primary and secondary stages of creep in constant load creep tests. The transient creep model predicts that the transient creep strain is dependent on stress and independent of test temperature. It is predicted that a true steady-state creep will only be observed after an infinitely long time. However, tertiary creep mechanisms are expected to intervene and lead to an acceleration in creep rate long before the onset of a true steady state. The model accurately predicts the strain *vs* time relationships for transient creep in IN738LC Ni-base superalloy, containing different grain boundary carbide distributions, over a range of temperatures.

## I. INTRODUCTION

IN constant load creep tests, the creep curve is divided into (1) primary, (2) secondary (steady state), and (3) tertiary regimes. The primary stage of creep is generally regarded as the transient stage of creep, and it has often been studied separately from the secondary creep.[1–7] However, Garofalo[8] and Dyson and McLean[9] have observed that in austenitic stainless steels and Ni-base superalloys under constant stresses (not constant loads), the transition between primary and secondary creep disappears and the transient creep is directly followed by tertiary creep. These observations indicate that creep is a continuous process, where a decreasing creep rate regime (transient creep) is followed by an accelerating creep rate regime (tertiary creep) beyond a minimum creep rate. It has also been pointed out that in constant load tests, it is more appropriate to consider the primary and secondary creep stages together as part of the transient creep regime.[10] The present article deals with grain boundary sliding (GBS) during the *primary plus secondary* stage of creep, which will be referred as the *transient* creep throughout the text.

In Ni-base superalloys, grain boundary carbides have been shown to decrease the creep rate by suppressing GBS.[11,12,13] Low stress creep test data generated on new and service-exposed IN738LC blades over a wide range of temperatures[11] indicate that upon changing the fine intragranular $\gamma'$ and discrete grain boundary carbide distributions to an overaged $\gamma'$ size and an almost continuous grain boundary carbide network as a result of service induced $\gamma'$ coarsening and MC carbide degeneration, respectively, the elastic strain normalized transient creep strain (the primary creep strain $\varepsilon_p$ plus the secondary creep strain $\varepsilon_s$) is significantly reduced relative to new blades over the entire range of test temperatures (Figure 1).[11] These observations indicate that grain boundary deformation processes must govern the transient creep behavior, considering that overaging of intragranular $\gamma'$ precipitates would decrease rather than increase resistance to creep deformation. The minimum creep rate data generated by Furrillo *et al.*[12] on NIMONIC* 115, in the presence and absence of grain boundary carbides, indicate that grain boundary carbides increase the apparent stress exponent from 2.18 to 14.58, whereas the activation energy increases from 334 KJ/mol (approximately the same as the activation energy for volume diffusion) to an apparent activation energy of 390 KJ/mol. A stress exponent of 2 matches favorably with the stress exponent value predicted by Langdon's GBS model,[14] which considers dislocation glide and climb in the grain boundary plane for clean planar boundaries. Furrillo *et al.*[12] rationalized this increase in stress exponent through the effect of a back stress resulting from carbides opposing dislocation motion in the grain boundary plane. The mechanistic significance of this data and rationale is that the transient creep in Ni-base superalloys, and perhaps most engineering alloys with the exception of columnar grained alloys and single crystal alloys, is controlled by GBS irrespective of test temperature and stress. This is not totally unexpected considering that in a polycrystalline material, stresses at geometrical discontinuities, such as the grain boundaries, will be higher than within the grain interiors, and dislocations at these locations will be activated immediately upon the application of a load during a creep test and will produce deformation.

*NIMONIC is a trademark of Inco Alloys International, Inc., Huntington, WV.

X.-J. WU, Visiting Fellow, and A.K. KOUL, Senior Research Officer, are with the Structures, Materials and Propulsion Laboratory, Institute for Aerospace Research, National Research Council of Canada, Ottawa, ON, Canada KIA OR6.

Manuscript submitted June 14, 1994.

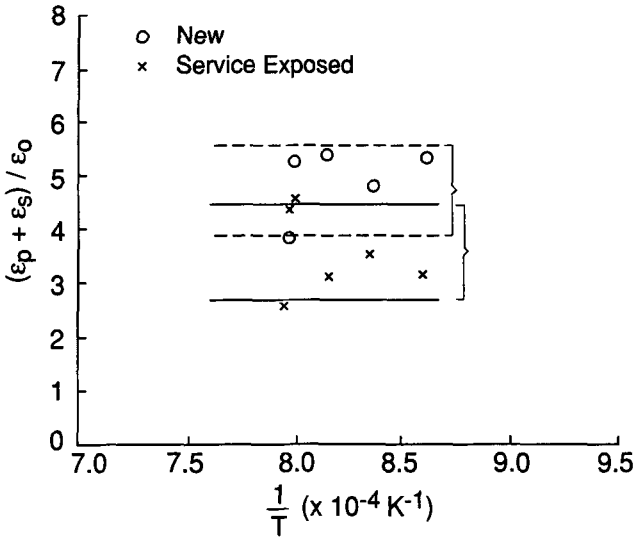


Fig. 1—Normalized transient strain varying as a function of temperature in new and service-exposed IN738LC blades at 90 MPa.

Some theoretical models for GBS for steady-state creep already exist in the literature.[14,15,16] However, these models do not take into account the presence of grain boundary precipitates or the back stresses opposing dislocation glide or climb. In dealing with transient creep, these models need to be modified to incorporate the back stresses, and most importantly, the evolutionary equations for back stresses need to be derived on a physical basis. It is the purpose of this article to provide a mathematical treatment for transient (combined primary and secondary) creep by considering that deformation is controlled by GBS.

## II. THE TRANSIENT CREEP MODEL

### A. *Review of Existing Transient Creep Models*

According to Malakondaiah *et al.*'s classification,[7] the primary creep models proposed to date can be grouped into (a) anelastic primary creep models (Burton and Reynolds,[1] Reynolds *et al.*,[2] and Raj and Ashby[3]), (b) primary creep models based on diffusion (Raj[5]) and (c) primary creep models based on intragranular dislocation annihilation (Burton[6] and Malakondaiah *et al.*[7]).

With respect to modeling transient (primary plus secondary) creep in the presence of grain boundary carbides, models based on intragranular dislocation annihilation are not applicable because dislocation annihilation is not likely to be the dominant process under GBS conditions. The anelastic sliding model developed by Raj and Ashby[3] and diffusion-based model developed by Raj[5] assume that the shear stress along the grain boundaries is relaxed and is equal to zero during the steady-state stage of creep. They only consider the influence of normal stress acting across the grain boundaries and regard sliding as an anelastic process accommodated by diffusional flow. Although this assumption disregards the localized stress equilibrium condition[17] at the grain boundaries, it could be used to describe diffusional flow processes for simplifying the analysis. Under GBS conditions, however, the influence of shear stress along the grain boundaries on plastic deformation cannot be ignored and the stress equilibrium condition must be satisfied at all times within a stressed body. An interface-reaction model has also been proposed by Arzt *et al.*[18] that takes into account the effects of grain boundary precipitates on diffusional processes leading to grain boundary migration through dislocation climb. This model is also not suitable for describing transient creep in the presence of grain boundary precipitates because (1) it ignores dislocation glide within the grain boundary plane, (2) the observed stress dependence of $\dot{\varepsilon}_m$ is greater than that predicted by interface-reaction-controlled diffusion, and (3) grain boundary migration has seldom been reported to occur in engineering alloys containing grain boundary precipitates.

In our view, grain boundary structural defects, such as ledges or defects introduced by grain boundary precipitates, can produce a self-balanced internal stress distribution, which may counteract the effect of applied stress locally. The component opposing the applied stress is often called the back stress. The concept of back stress is well established in constitutive modeling of plastic deformation.[19–24] Back stresses for constant structures have been given in some forms, such as Peierls stress (for lattice friction) and Orowan stress (in the presence of precipitates), or related to the total dislocation density (the number of primary dislocations plus forest dislocations) by Seeger.[21] However, the problem of dealing with time-dependent back stresses in grain boundary planes has yet to be addressed. In this respect, new creep models are needed to deal with transient creep (primary creep plus secondary creep) under GBS conditions.

In our theoretical treatment, we adopt Langdon's physical premise[14] but modify the model to include the effects of back stresses opposing dislocation glide and climb in the grain boundary plane in the presence of grain-boundary precipitates. We consider that the back stress opposing dislocation glide arises from dislocation pileups that form at all grain-boundary precipitate intersections and use Arzt and Rösler's solution[25,26] to represent the back stress that restricts dislocation climb. The evolution of back stresses will be derived from the kinetics of dislocation pileups in the following sections.

### B. *Dislocation Glide in the Presence of Grain Boundary Precipitates*

We consider a planar grain boundary containing uniformly distributed grain boundary precipitates (Figure 2). For simplicity of treatment, we assume that these grain boundary precipitates are elliptical particles with a height of $r$ and interparticle spacing of $\lambda$. Grain boundary dislocations move between these particles under the applied stress $\tau$ and pile up when they are blocked at the edge of a particle. Suppose, at time $t$, there are $n$ pileup dislocations at the edge of a particle. These pileup dislocations together will exert a back

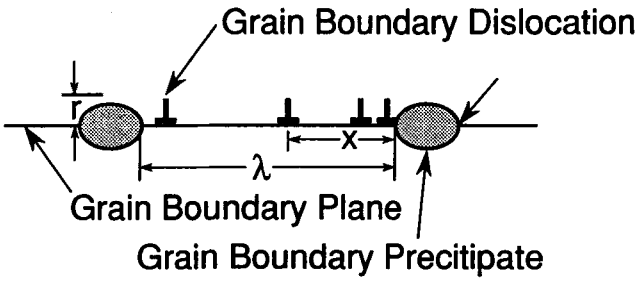


Fig. 2—A schematic of dislocation pileups at the edge of a particle.

stress on a moving dislocation located at a distance $x$ from the particle.[27]

$$\tau_b(x) = \frac{n\mu\mathbf{b}}{2\pi(1-\nu)x} \quad [1]$$

where $\nu$ is the Poisson's ratio, $\mathbf{b}$ is the Burgers vector, and $\mu$ is the elastic shear modulus. Therefore, for a dislocation to glide over a distance $\lambda$, the applied work, $\tau\lambda$, must overcome the resistance work represented by the integration of Eq. [1] over the moving distance $\lambda$:

$$\tau\lambda \geq \int_{n\mathbf{b}}^{\lambda} \tau_b(x)dx \quad [2]$$

From this, an average back stress opposing dislocation glide, $\tau_{ig}$, can be defined as

$$\tau_{ig} = \frac{1}{\lambda}\int_{nb}^{\lambda} \tau_b(x)dx \quad [3]$$

Substituting Eq. [1] into Eq. [3] yields

$$\tau_{ig} = \frac{n\mu\mathbf{b}}{2\pi(1-\nu)\lambda}\ln\frac{\lambda}{n\mathbf{b}} \quad [4]$$

The change in the number of pileup dislocations can be accounted for by subtracting the number of dislocations climbing over the obstacle from the number of dislocations arriving at the obstacle. Let $\rho$ be the dislocation density, $v$ be the average dislocation glide velocity, and $\kappa$ be the rate of climb. The number of new dislocations arriving per unit time is given by $\rho vr$, and the number of dislocations leaving is equal to $n\kappa$. Hence, the change in the number of pileup dislocations is given by

$$\frac{dn}{dt} = \rho vr - n\kappa = \frac{r}{\mathbf{b}}(\rho\mathbf{b}v) - n\kappa \quad [5]$$

Using the Orowan equation[28] $\dot{\gamma} = \rho bv$, Eq. [5] can be written into

$$\frac{dn}{dt} = \frac{r}{\mathbf{b}}\dot{\gamma} - n\kappa \quad [6]$$

Upon differentiating Eq. [4] and using Eq. [6], the evolutionary equation for $\tau_{ig}$ is obtained as

$$\frac{d\tau_{ig}}{dt} = \frac{\mu\mathbf{b}}{2\pi(1-\nu)\lambda}\left[\ln\left(\frac{\lambda}{n\mathbf{b}}\right) - 1\right]\left(\frac{r}{\mathbf{b}}\dot{\gamma} - n\kappa\right) \quad [7]$$

Usually, the precipitate spacing $\lambda$ is on the order of microns, but a Burgers vector is less than half of a nanometer. For simplifying Eq. [7], we can assume $\ln(\lambda/n\mathbf{b}) \gg 1$, and hence, Eq. [7] can be written in the form

$$\frac{d\tau_{ig}}{dt} = H\dot{\gamma} - \kappa\tau_{ig} \quad [8]$$

where $H = [\mu r/2\pi(1-\nu)\lambda]\ln(\lambda/n\mathbf{b})$ is the work-hardening coefficient. The term $\tau_{ig}\kappa$ in Eq. [8] represents the recovery rate controlled by dislocation climb. Equation [8] follows the well-known Bailey-Orowan type hardening-recovery formalism.[19,20] According to Eq. [8], the work-hardening coefficient, $H$, varies slightly with the number of pileup dislocations during transient creep. For the convenience of mathematical treatment, we ignore the logarithm variation of $n$ (or $\tau_{ig}$) and modify the work-hardening coefficient into the form

$$H = \frac{\xi\mu r}{2\pi(1-\nu)\lambda}\ln\frac{\lambda}{\mathbf{b}} \quad [9]$$

where $\xi$ $(0 < \xi < 1)$ is a modification factor.

### C. *Dislocation Climb in the Presence of Grain Boundary Precipitates*

To consider the influence of grain boundary precipitates on dislocation climb, the migration of vacancies along the grain boundary plane must be addressed first. We consider an edge dislocation lying at the center of its glide plane (Figure 3). Using Volterra's solution,[27] the hydrostatic pressure in the upper half plane is given by

$$p(\rho,\theta) = \frac{1}{3}(\sigma_x + \sigma_y + \sigma_z) = -\frac{(1+\nu)\mu\mathbf{b}}{3\pi(1-\nu)}\rho^{-1}\sin\theta \quad [10]$$

Suppose a vacancy is forced to migrate from the position $(\rho, \theta)$ to the dislocation core, the preferred path for vacancy migration is the path that expends the least energy, as indicated in Figure 3. It can easily be proven that the minimum energy required is

$$W_{\min} = -\int_S p(\rho,\theta)\mathbf{b}^2 ds = \int_0^{\theta}\frac{(1+\nu)\mu\mathbf{b}^3}{3\pi(1-\nu)}\rho^{-1}\sin\theta(\rho d\theta) = \frac{(1+\nu)\mu\mathbf{b}^3}{3\pi(1-\nu)}(1-\cos\theta) \quad [11]$$

where $ds = \rho d\theta$ in Figure 3.

Assume that dislocations are perfect sinks of vacancies and a dislocation climbs a Burgers vector when it absorbs vacancies (in the two-dimensional plane, Figure 3). Since one side of the grain boundary precipitates, such as carbides, is usually coherent with the

matrix of the parent grain, we need only to consider dislocation climb along the noncoherent side of the precipitate particle. This means that we can treat the problem in the upper half plane in Figure 3. In the presence of grain boundary precipitates, the minimum work needed to transport a vacancy to the dislocation core is

$$W_{min} = \frac{(1+\nu)\mu\mathbf{b}^3}{3\pi(1-\nu)}(1-\cos\theta_{min}) = \frac{(1+\nu)\mu\mathbf{b}^3}{3\pi(1-\nu)}\left(1-\frac{\lambda}{\sqrt{\lambda^2+r^2}}\right) \quad [12]$$

Thus, additional work, $\Delta U = W_{min}$, must be compensated by additional thermal energy such that vacancies can migrate to cause dislocation climb in the presence of grain boundary precipitates. The total activation energy for dislocation climb is hence equal to the activation energy for diffusion along clean boundaries, $U_d$, plus an additional energy, as given by Eq. [12]:

$$U_c = U_d + \Delta U = U_d + \frac{(1+\nu)\mu\mathbf{b}^3}{3\pi(1-\nu)}\left(1-\frac{\lambda}{\sqrt{\lambda^2+r^2}}\right) \quad [13]$$

Hence, the diffusion coefficient should be modified as

$$D = b^2\nu_0\exp\left(-\frac{U_c}{kT}\right) = \mathbf{b}^2\nu_0\exp\left(-\frac{U_d+\Delta U}{kT}\right) \quad [14]$$

where $\nu_0$ is the atomic frequency.

According to Arzt and Rösler,[25,26] when a dislocation climbs along the particle/matrix interface, the dislocation-particle interaction will produce a back stress $\sigma_{ic}$, which reduces the effective stress, acting on a climbing dislocation, to $\sigma - \sigma_{ic}$. This back stress, $\sigma_{ic}$, is independent of time and is given by

$$\sigma_{ic} = \frac{\alpha\mu\mathbf{b}}{\lambda} \quad [15]$$

where $\alpha$ is a factor less than unity, the value of which depends on the degree of coherency of the precipitate particle.

Therefore, in the presence of grain boundary precipitates, the rate of vacancy diffusion should be described by

$$\kappa = \frac{D\mu\mathbf{b}}{kT}\frac{\sigma-\sigma_{ic}}{\mu} = \frac{\sqrt{3}D\mu\mathbf{b}}{kT}\frac{\tau-\tau_{ic}}{\mu} \quad [16]$$

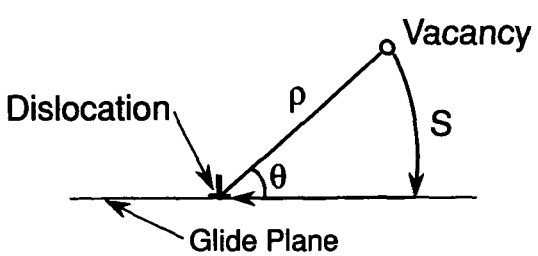


Fig. 3—Vacancy migration in the stress field of an edge dislocation.

where $\sigma_{ic}$ and $\tau_{ic}$ are, respectively, the normal and shear components of back stress obtained by Rösler and Arzt,[25,26] according to the relation $\sigma = \sqrt{3}\tau$.

### D. *The Modified Langdon's Model for GBS*

In presenting a rate equation for GBS, we modify Langdon's model[14] as follows. As assumed by Langdon, if GBS occurs by the glide and climb of grain-boundary dislocations, the rate of GBS is governed by the rate of climb since climb is a slower process. According to Langdon[14], the rate of climb, $\dot{s}$, along the boundary is given

$$\dot{s} = N\mathbf{b}\kappa \quad [17]$$

where $N$ is the number of grain boundary dislocations per unit length.

The number of dislocations per unit length in a grain boundary can be related to the effective shear stress, $\tau - \tau_{ig}$ (in Langdon's model for clean boundaries[14] $\tau_{ig} = 0$), in the form of

$$N = \frac{2\pi(1-\nu)(\tau-\tau_{ig})}{\mu\mathbf{b}} \quad [18]$$

The shear strain rate produced by combined dislocation climb and glide processes along a grain boundary plane, $\dot{\gamma}_{GBS}$, is[14]

$$\dot{\gamma}_{GBS} = MA\mathbf{b}\dot{s} \quad [19]$$

where $M$ ($M \sim 6/\pi d^3$) is the number of boundaries per unit volume, $d$ is the grain size, and $A$ is the total area swept out by dislocations moving along the boundary. Langdon assumed $A \sim \pi d^2$ for clean grain boundaries. But, in the presence of grain boundary precipitates, $A$ cannot be the area of a whole grain boundary facet swept by dislocations. Instead, $A$ should be proportional to $(\lambda + r)d$ in the presence of a discrete grain boundary particle distribution and proportional to $\pi(\lambda + r)^2$ in the presence of a continuous particle network, as schematically shown in Figures 4(a) (adopted from Arzt *et al.*[18]) and (b), respectively.

Substituting Eqs. [16] through [18] into Eq. [19] and

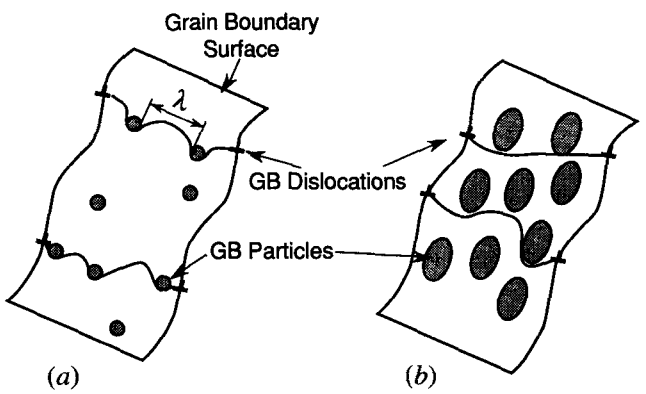


Fig. 4—Schematic of grain boundary carbide distribution: (*a*) discrete carbides (adopted from Arzt *et al.*[18]) and (*b*) an almost continuous network of carbides.

considering all the possible dependences of $A$, we can obtain the following

$$\dot{\gamma}_{GBS} \sim 12\pi\sqrt{3}(1-\nu) \cdot \left(\frac{\mathbf{b}}{d}, \frac{(\lambda+r)\mathbf{b}}{\pi d^2}, \frac{(\lambda+r)^2\mathbf{b}}{d^3}\right) \frac{D\mu\mathbf{b}}{kT} \frac{(\tau-\tau_{ig})(\tau-\tau_{ic})}{\mu^2} \quad [20]$$

Therefore, the GBS-controlled plastic strain rate can be written in an abbreviated form:

$$\dot{\gamma}_{GBS} = A_0 \frac{D\mu\mathbf{b}}{kT} \left(\frac{\mathbf{b}}{d}\right)^q \left(\frac{\lambda+r}{\mathbf{b}}\right)^{q-1} \frac{(\tau-\tau_{ig})(\tau-\tau_{ic})}{\mu^2} \quad [21]$$

where $A_0$ is a nondimensional constant and $q$ is the grain size index, which takes values of 1 (without particles), 2 (discrete particles), and 3 (continuous network of particles). In the absence of grain boundary precipitates, $\lambda$ will be equal to the interledge spacing and $r$ will approach the average grain boundary ledge height. In modifying Langdon's model, we have assumed that grain-boundary ledges have negligible effect on dislocation glide and climb relative to grain-boundary carbides.

### E. *The Transient Creep Strain Equation*

During transient creep, plastic deformation is governed by the rate equation (Eq. [21]) and an evolutionary equation (Eq. [8]) for $\tau_{ig}$ only since $\tau_{ic}$ is time independent.

Substituting Eq. [21] into Eq. [8] results in

$$\frac{d\tau_{ig}}{dt} = HA_1(\tau-\tau_{ig})(\tau-\tau_{ic}) - \tau_{ig}\kappa$$

$$= HA_1(\tau-\tau_{ic})\left[\tau - \left(1 + \frac{\kappa}{HA_1(\tau-\tau_{ic})}\right)\tau_{ig}\right]$$

$$= \eta(\tau - \beta\tau_{ig}) \quad [22]$$

where

$$A_1 = A_0 \frac{D\mathbf{b}}{\mu kT}\left(\frac{b}{d}\right)^q \left(\frac{\lambda+r}{\mathbf{b}}\right)^{q-1},$$

$$\eta = HA_1(\tau-\tau_{ic}), \qquad \beta = 1 + \frac{\kappa}{\eta} \quad [23]$$

The solution of the differential equation (Eq. [22]) takes the form

$$\tau_{ig} = \frac{\tau}{\beta}[1 - \exp(-\eta\beta t)] \quad [24]$$

with a steady-state ($t \to \infty$) value of $\tau_{i\infty} = \tau/\beta$.

Substituting Eq. [24] into Eq. [21], the transient creep strain can be integrated as

$$\gamma = \gamma_0 + \dot{\gamma}_{ss}t + \frac{\tau}{H\beta^2}[1 - \exp(-\eta\beta t)] \quad [25]$$

where $\gamma_0$ is the initial strain and

$$\dot{\gamma}_{ss} = A_1(\tau-\tau_{i\infty})(\tau-\tau_{ic}) \quad [26]$$

is the steady-state creep rate.

## III. DISCUSSION

The present model, as expressed in the context of Eqs. [8] and [21], treats transient creep as a GBS phenomenon that is influenced by the evolution of back stresses associated with the presence of grain-boundary precipitates. The evolutionary equation for internal stress opposing glide is derived from the kinetics of dislocation pileups and, therefore, provides a physical description for the change in structure during creep deformation. According to Eq. [25], true steady-state creep occurs after an infinitely long time. However, long before the onset of true steady state, tertiary creep due to cavity nucleation and growth processes will take over and lead to an acceleration in the creep rate. Rigorously speaking, the observed steady-state creep is always a part of the transient creep. The distinction between the primary stage and the apparent secondary stage in constant load tests bears no physical significance, although the definition provides an engineering convenience to evaluate an approximate value of the steady-state creep rate.

From an engineering point of view, the steady-state creep rate equation (Eq. [26]) can be used to describe the experimentally observed minimum creep rate ($\dot{\gamma}_m$ or $\dot{\varepsilon}_m$) data. Furrillo *et al.* observed a stress exponent of 2 for $\dot{\varepsilon}_m$ in specimens without grain-boundary carbides and 14.58 in specimens with grain-boundary carbides.[12] Although they empirically accounted for this increase in the stress exponent by considering the effect of back stress induced by the presence of grain boundary carbides, they did not distinguish between the mechanistic roles that grain-boundary carbides play in dislocation glide and climb processes. Equation [26] correlates the creep rate with an effective stress for glide, $(\tau - \tau_{ig})$, and an effective stress for climb, $(\tau - \tau_{ic})$. Upon plotting Furrillo *et al.*'s $\dot{\varepsilon}_m$ data for carbide-free and carbide-containing microstructures of NIMONIC 115 against the product of these two components of stresses on a log-log scale, the data are well represented by two parallel lines with a slope of unity for both cases, (Figure 5). This confirms that the present GBS model accurately predicts the stress dependence of $\dot{\varepsilon}_m$ in the presence of grain-boundary carbides.

As regards the temperature dependence of NIMONIC 115 $\dot{\varepsilon}_m$ data, Furrillo *et al.*[12] found that at high stresses (517 to 568 MPa) and moderate temperatures (746 to 788 °C), the deformation was controlled by volume diffusion with an activation energy of 334 KJ/mol in specimens without grain-boundary carbides, whereas the activation energy increased to 390 KJ/mol in specimens with grain-boundary carbides. An increase in activation energy would be expected to occur in the presence of carbides, because additional thermal energy is needed for vacancies to diffuse along grain boundaries such that dislocations can climb over the carbides. The additional activation energy ($\Delta U$) can be calculated through Eq. [12]. Using $\lambda$ and $r$ values for NIMONIC 115,[12] the $\Delta U$ is calculated to be 45.7 KJ/mol (Table I). Therefore, according to our theoretical model, the total activation energy for creep in NIMONIC 115 should be 380.1 (334.4 + 45.7) KJ/mol, which agrees well with Furrillo *et al.*'s observation, although the predicted value is lower than the experimental value by 10 KJ/mol.

**Table I. Activation Energy Data for NIMONIC 115 and IN738LC Ni-Base Superalloy Materials**

| Material | Carbide Size and Spacing, $\mu$m | Experimental $U_c$, KJ/mol | Reference $U_d$, KJ/mol | Theoretical $\Delta U$, KJ/mol |
|---|---|---|---|---|
| NIMONIC 115 | $r = 0, \quad \lambda = \infty$ | 334.4[12] | 334.4 | 0 |
| $\mu$ = 75 GPa | $r = 2.5, \lambda = 2$ | 390.4[12] | 334.4 | 45.7 |
| $b = 2.4 \times 10^{-10}$ m | | | | |
| IN738LC | | | | |
| $\mu$ = 72 GPa | | | | |
| $b = 2.4 \times 10^{-10}$ m | | | | |
| New | $r = 0.4, \lambda = 1.5$ | 230 (LT) | 222 (LT) | 8.4 |
| | | 480 (HT) | 472 (HT) | 8.4 |
| Service exposed | $r = 0.7, \lambda = 0.7$ | 250 (LT) | 222 (LT) | 34.5 |
| | | 500 (HT) | 472 (HT) | 34.5 |

Castillo *et al.*[11] have generated low stress (90 MPa) $\dot{\varepsilon}_m$ data on new and service-exposed IN738LC turbine blade materials over a range of temperatures varying between 899 °C and 988 °C (Figure 6). The new material contained discrete grain-boundary carbides, whereas the service-exposed material contained an almost continuous network of grain-boundary carbides. Average carbide radius and intercarbide spacing values for both materials are given in Table I. It was observed that for the new material, the apparent activation energy was 230 KJ/mol below a transition temperature of 950 °C and the activation energy was 480 KJ/mol above this transition temperature (Figure 6). In the case of the service-exposed material, the apparent activation energy increases to 250 KJ/mol below 950 °C and to 500 KJ/mol above 950 °C. Even though these experimental activation energy values are considerably higher than those reported for grain-boundary diffusion (115 KJ/mol) and volume diffusion (334 KJ/mol) in Ni-base superalloys, it is believed that grain-boundary diffusion and lattice diffusion, respectively, control the creep processes below and above this transition temperature, and the reason for these differences will be explained subsequently.

An interesting feature of the IN738LC data described by Castillo *et al.*[11] is that upon changing the discrete carbides to continuous network, the activation energies, both below and above the transition temperature, increase by approximately 20 KJ/mol, (Figure 6). This

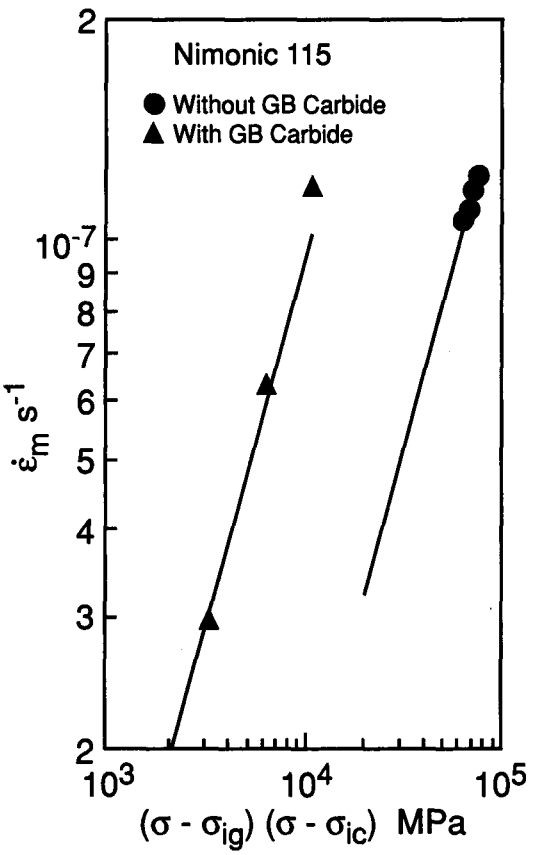


Fig. 5—The minimum creep rate $\dot{\varepsilon}_m$ *vs* the multiplication of $(\sigma - \sigma_{ig})$ and $(\sigma - \sigma_{ic})$ in NIMONIC 115. For the material with grain boundary carbides, $\sigma_{ig} = \sigma/\beta$, $\beta = 1.3$, and $\sigma_{ic} = 487$ MPa. The $\dot{\varepsilon}_m$ data are taken from Furrillo *et al.*[12] The solid lines represent the linear regressions.

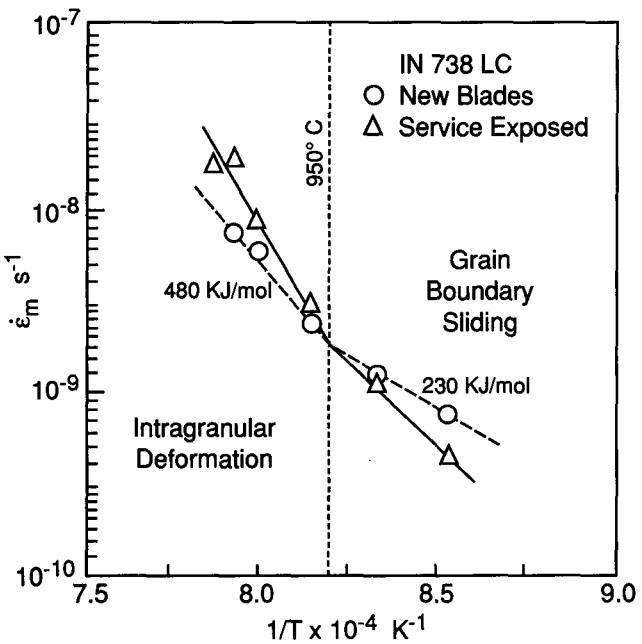


Fig. 6—The minimum creep rate of $\dot{\varepsilon}_m$ varying as a function of temperature in new and service-exposed IN738LC blades at 90 MPa. The symbols represent the observed $\dot{\varepsilon}_m$ data.[11]

increase in activation energy, $\Delta U$, is close to a $\Delta U$ value of 26 (34.4 − 8.4) KJ/mol predicted through Eq. [12]. Again, relative to discrete carbides, additional thermal energy is needed for dislocations to climb over larger and more closely spaced carbides (Table I). This analysis therefore indicates that the proposed GBS model adequately accounts for the role of carbides on temperature dependence of dislocation climb in complex engineering alloys.

Upon correcting for $\Delta U$ arising from dislocation climb in the presence of discrete and continuous carbides in new and service-exposed IN738LC blades (Table I), the corrected apparent activation energy assumes a value of 472 KJ/mol above 950 °C and 222 KJ/mol below 950 °C for both materials. These corrected activation energy values are considerably larger than those expected for lattice diffusion (334 KJ/mol) and grain-boundary diffusion (115 KJ/mol) in Ni-base superalloys. In fact, the difference between the corrected activation energy and theoretical activation energy is 138 KJ/mol, in the temperature range of 960 to 990 °C, and 107 KJ/mol, in the temperature range of 899 to 930 °C, tested at a low stress of 90 MPa. It will be recalled that in NIMONIC 115, tested in the lower temperature range of 746 to 788 °C at a stress of 517 MPa, the difference between the corrected and theoretical activation energy is only about 10 KJ/mol. These results indicate that the difference between the corrected and theoretical activation energies decreases considerably with increasing stress. This trend suggests that another deformation mechanism is contributing to temperature dependence of $\dot{\varepsilon}_m$ in the presence of grain-boundary carbides. Atomistically, the energy barrier introduced by this deformation mechanism is small at high stresses and quite large at low stresses. A possible explanation is that a limited amount of cavity nucleation might occur concurrently with dislocation glide and climb, which eventually leads to the onset of tertiary creep (where the minimum creep rate is measured). According to the analysis of Raj and Ashby,[29] cavity nucleation requires an additional thermal energy that is equal to $4\Gamma^3 F_v/\sigma^2$, where $\Gamma$ is the surface energy and $F_v$ is the shape factor of cavities. From this expression, it is expected that the apparent activation energy will be lower at higher stresses and *vice versa*. This is perhaps the reason why anomalous activation energies were observed in the case of IN738LC specimens because the tests were conducted at a low stress (90 MPa). In contrast, the NIMONIC 115 data was generated at a considerably high stress (517 MPa), where the energy barrier for cavity nucleation is considerably lower and the corrected activation energy is close to the activation energy for volume diffusion in Ni-base superalloys.

The present model describes the transient creep strain and time relationship through Eq. [25], where the rate parameter $\eta$ can be expressed as

$$\eta = HA_1(\tau - \tau_{ic}) = \frac{H\dot{\gamma}_{ss}}{\tau - \tau_{i\infty}} = \frac{\beta^2 H\dot{\gamma}_{ss}}{\tau(\beta - 1)} \qquad [27]$$

Upon transforming the shear components ($\tau$, $\gamma$, $\mu$) into tensile components ($\sigma$, $\varepsilon$, $E$), Eq. [25] takes the form

$$\varepsilon = \varepsilon_0 + \dot{\varepsilon}_m t + \frac{\sigma}{\beta^2 H}\left[1 - \exp\left(-\frac{\beta^2 H\dot{\varepsilon}_m t}{\sigma(\beta - 1)}\right)\right] \qquad [28]$$

It is interesting to note that Eq. [28] takes the same form as the empirical creep strain equation proposed by Garofalo[8] many years ago. This strain behavior has been test proven in many alloy systems.[8] However, unlike Garofalo's empirical model, Eq. [28] provides a mechanistic interpretation of the primary and the secondary stages of creep. The transient creep strain is shown to consist of two time-variant components: the primary strain component, which will saturate to its maximum value exponentially with increasing time, and the secondary strain component, which increases linearly with time. With regard to the primary creep, the model predicts that the maximum primary strain $\varepsilon_{tr}^p$, where the primary strain is defined as the total plastic strain in the transient regime minus the secondary strain, $\dot{\varepsilon}_m t$, increases linearly with stress and is given by

$$\varepsilon_{tr}^p = \frac{\sigma}{\beta^2 H} \qquad [29]$$

The primary creep time, where the primary time is defined as the time required to attain 99 pct of the maximum primary strain, $\varepsilon_{tr}^p$, follows the relationship

$$t_{tr}^p = 4.6\frac{(\beta - 1)\sigma}{\beta^2 H\dot{\varepsilon}_m} = \frac{4.6\mu}{\beta H}\frac{kT}{Db(\sigma - \sigma_{ic})}\left(\frac{d}{b}\right)^q\left(\frac{b}{\lambda + r}\right)^{q-1} \qquad [30]$$

Note that the preceding definition of the primary strain is different from the conventional definition in engineering, where the primary strain is defined, arbitrarily to some extent, by the first deflection point below the secondary stage of a creep curve. To clear the confusion in these definitions, a nomenclature is given in Appendix A. According to Eq. [29], the maximum primary strain normalized by the elastic strain ($\varepsilon_0 = \sigma/\mu$) is independent of stress, temperature, and grain size. According to Eq. [30], the primary time is inversely proportional to the diffusional constant $D$ and could vary with the grain size up to the third power, depending upon the morphology and distribution of grain-boundary precipitates. These predictions of Eq. [28] are consistent with numerous observations in a number of materials, as reviewed by Malakondaiah *et al.*[7] In cases where grain-boundary precipitates are absent, the influence of grain-boundary ledges on grain-boundary dislocation movement would have to be considered in detail. In such analyses, the relationship between grain-boundary ledge density and grain size would have to be incorporated in the previous equations.

In the case of new and service-exposed IN738LC blades, structural parameters, $\beta$ and $H$, for the two material conditions can be obtained by solving Eqs. [29] and [30], where the maximum primary strain, $\varepsilon_{tr}^p$, and the primary time, $t_{tr}^p$, are measured from creep tests. Based on the short-term creep data at 954 °C, $\beta$ was estimated to be 1.313 and 1.13 and $H$ was estimated to be 18 and 30 GPa for new and service-exposed materials, respectively (an example of calculation is given in Appendix B). These values together with the creep test data are given in Table II. Then the values of $\dot{\varepsilon}_m$, $\beta$, and

**Table II. Values of Different Parameters Used in Equation [28] to Compute IN738LC Creep Curves at a Creep Stress of 90 MPa in Figures 7 and 8**

| IN738LC Material Condition | Test Temperature | $E/E_0$* | $\varepsilon_0$ (Pct) | $\beta$ | $H$ (GPa) | $\dot{\varepsilon}_m$ ($10^{-9}$ $s^{-1}$) |
|---|---|---|---|---|---|---|
| New | 954 °C | 0.70 | 0.1 | 1.313 | 18.0 | 2.0 |
| New | 899 °C | 0.719 | 0.24 | 1.313 | 18.0 | 0.73 |
| 14,159 h of service | 954 °C | 0.70 | 0.45 | 1.13 | 30.0 | 3.05 |
| 30,600 h of service | 899 °C | 0.719 | 0.36 | 1.13 | 30.0 | 0.46 |

*Note: $E_0$ = 200 GPa.

$H$ are substituted into Eq. [28] to compute transient creep curves for both new and service-exposed blades, (Figure 7). The descriptions of Eq. [28] agree very well with the experimental data in the transient regime. The same parameters $\beta$ and $H$ are then used to predict the transient behaviors of both new and service-exposed materials in long-term creep tests at 899 °C. The predictions of Eq. [28] also agree very well with the observed behaviors at 899 °C (Figure 8) Figures 7 and 8 clearly show that Eq. [28] can be used to describe the transient creep behavior of complex engineering alloys in both short- and long-term creep tests. Equation [28] in its present form predicts a transient time of infinity, although a tertiary creep mechanism resulting in extensive cavity nucleation and growth will obviously intervene at some stage of the transient to accelerate the creep rate and cause final fracture. Therefore, Eq. [28] will have to be coupled with an appropriate tertiary creep equation in order to predict the entire creep curve and the rupture life. This work is currently in progress in the authors' laboratory and will form the subject of another article.

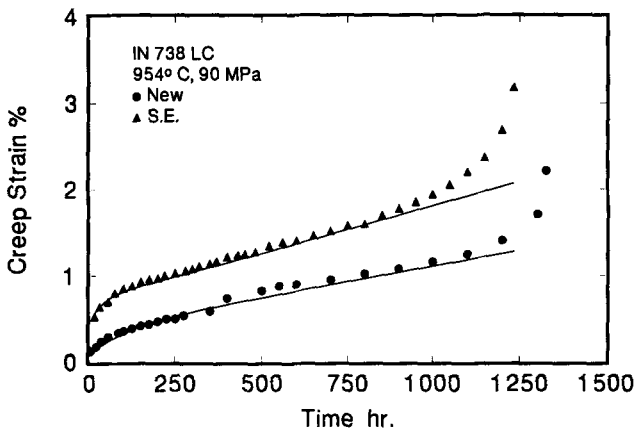


Fig. 7—Creep strain *vs* time relationship for new and service-exposed IN738LC blades tested at 954 °C and 90 MPa. The symbols represent the test data.[11] The solid lines represent the predictions from Eq. [28] using parameters given in Table II.

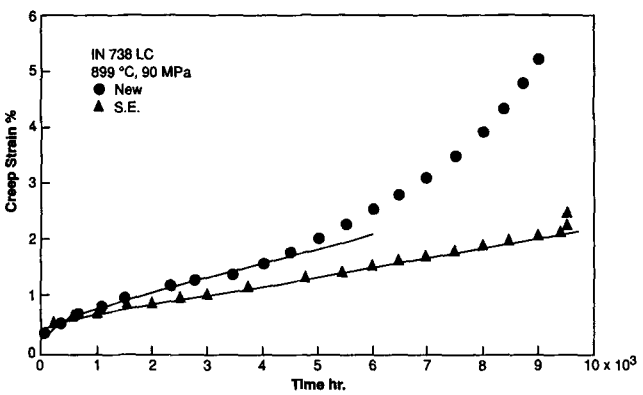


Fig. 8—Creep strain *vs* time relationship for new and service-exposed IN738LC blades tested at 899 °C and 90 MPa. The symbols represent the test data.[11] The solid lines represent the predictions from Eq. [28] using parameters given in Table II.

In Figure 1, we presented normalized transient strain ($\varepsilon_p + \varepsilon_s$) data, where it was shown that $\varepsilon_{tr}$ is independent of temperature for both new and service-exposed IN738LC blade materials. Theoretically, given the percentage, $P$ ($P$ can be chosen arbitrarily close to unity to cover the whole transient regime), at which the primary strain is attained relative to its maximum value, the transient creep strain can be expressed as

$$\varepsilon_{tr} = \varepsilon_0 - \ln(1 - P)\frac{\sigma(\beta - 1)}{\beta^2 H} + P\frac{\sigma}{\beta^2 H} \quad [31]$$

which, if normalized by $\varepsilon_0 = \sigma/\mu$, should be independent of temperature. Equation [31] also predicts that the elastic strain normalized transient strain in a highly work-hardenable material, which corresponds to material containing a dense population of grain-boundary precipitates, is lower than in a low work-hardenable material, which corresponds to a material containing sparse grain-boundary precipitate distribution. In real creep tests, the time to measure the transient creep strain will depend on when tertiary creep takes over from the transient stage. Anyway, a tertiary creep formalism will be needed to describe the entire creep process.

## IV. CONCLUSIONS

A theoretical treatment for GBS in the presence of grain boundary precipitates is presented. A constitutive equation is developed by modifying Langdon's grain boundary sliding model and by incorporating back stresses opposing dislocation glide ($\tau_{ig}$) and climb ($\tau_{ic}$). An evolutionary equation for $\tau_{ig}$ is derived by considering the kinetics of dislocation pileups at the edge of a precipitate particle. The influence of grain-boundary precipitates on dislocation climb is considered by (1) accounting for the additional thermal energy required for vacancies to diffuse to the cores of dislocations held by precipitate particles and (2) direct particle-dislocation

interactions resulting in an Orowan-type back stress. The modified rate equation for GBS takes the form

$$\dot{\gamma}_{GBS} = \frac{A_1(D\mu b)}{kT}\left(\frac{b}{d}\right)^q \left(\frac{\lambda + r}{b}\right)^{q-1} \frac{(\tau - \tau_{ig})(\tau - \tau_{ic})}{\mu^2}$$

where $q$ is the grain size index, which assumes values of 1 for clean boundaries, 2 for a discrete precipitate distribution and 3 for an almost continuous precipitate network. This rate equation accurately describes the stress dependence of minimum creep rate in engineering alloys containing grain boundary precipitates. The diffusion coefficient $D$ has been modified into the form

$$D = b^2\nu_0 \exp\left(-\frac{U_d + \Delta U}{kT}\right)$$

where $\Delta U$ is an additional activation energy term arising from the presence of grain boundary precipitates and $U_d$ is the diffusional activation energy for clean grain boundaries. An expression for $\Delta U$ is derived, which accurately predicts the change in experimental activation energies when a discrete grain boundary carbide distribution is changed to a continuous network of grain boundary carbides in IN738LC Ni-base superalloys and when comparing the results obtained by other workers on clean grain boundaries and carbide containing grain boundaries in NIMONIC 115 Ni-base superalloy.

Upon integrating the GBS rate equation and coupling it with the physically based expressions for $\tau_{ig}$ and $\tau_{ic}$, an equation for transient creep (primary plus secondary stage), in terms of strain as a function of time, is derived. The transient creep equation for a given temperature takes the form

$$\gamma = \gamma_0 + \dot{\gamma}_{ss}t + \frac{\tau}{H\beta^2}[1 - \exp(-\eta\beta t)]$$

where $\beta$ is a material constant, $H$ is the work-hardening coefficient, and $\eta$ is a parameter relating to the rate of dislocation climb. This transient strain equation is very similar to Garofalo's empirical equation, and it accurately predicts the transient creep behavior of IN738LC Ni-base superalloy material containing a discrete carbide distribution or a continuous network of carbides. The model also predicts that the maximum primary creep strain increases with stress and is independent of temperature. The transient creep model in its present form predicts that a true steady-state creep occurs after an infinitely long time, although some cavitation mechanism leading to tertiary creep is expected to intervene long before the onset of the steady state. The present transient creep model needs to be coupled with an appropriate tertiary creep model to predict the entire creep behavior of complex engineering alloys. Our analysis of $\dot{\varepsilon}_m$ data on IN738LC and NIMONIC 115 Ni-base superalloys indicates that in the presence of grain boundary carbides, a limited amount of cavity nucleation probably occurs prior to the onset of tertiary creep, which leads to an increase in the observed activation energy relative to the theoretical activation energy for diffusion at high temperatures. The difference between theoretical and experimental activation energies decreases with increasing stress and decreasing temperature.

## APPENDIX A

### Nomenclature of transient creep

Referring to a typical creep curve shown in Figure A1, strain components in the transient regime are defined as follows.

$\varepsilon_0$ Initial strain; theoretically, $\varepsilon_0 = \sigma/E$, but the measurement may include a misfit displacement in the grip system.

$\varepsilon_p$ Engineering primary strain, defined by the first deflection point below the linear portion of the creep curve.

$\varepsilon_s$ Engineering secondary strain, the strain increment which is linearly proportional to time after the primary stage.

$\varepsilon_{tr}^p$ The maximum primary strain component in the transient regime.

$\varepsilon_{tr}^s$ The steady-state strain component in the transient regime.

In the literature,[7] $\varepsilon_{tr}^p$ is often called the transient strain, which is really a measure of the primary stage. Since we consider the transient regime as the combination of the primary and the secondary stages, the transient strain should be expressed as

$$\varepsilon_{tr} = \varepsilon_p + \varepsilon_g = \varepsilon_0 + \varepsilon_{tr}^p + \varepsilon_{tr}^s$$

## APPENDIX B

### Evaluation of $\beta$ and $H$

Take the creep test of a new blade specimen at 954 °C, for example, $\sigma = 90$ MPa, $\dot{\varepsilon}_m = 2 \times 10^{-9}$ s$^{-1}$, the primary time, $t_p$, was measured to be 579 hours and the maximum primary strain, $\varepsilon_{tr}^p$, was measured to be 0.0029. Substituting these values into Eqs. [29] and [30] results in

$$\varepsilon_{tr}^p = \frac{\sigma}{\beta^2 H} = 0.0029 \qquad [B1]$$

and

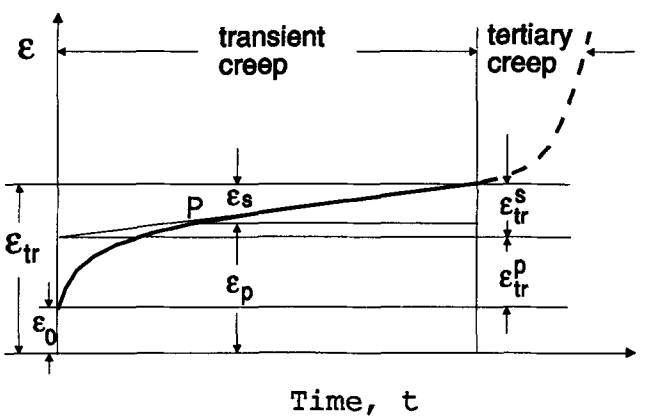


Fig. A1—Typical creep curve and the definition of transient strain. The term $P$ indicates the point where the engineering primary strain could be measured.

$$t_{tr}^{p} = 4.6\frac{(\beta - 1)\sigma}{\beta^2 H\dot{\varepsilon}_m} = 2{,}084{,}400 \quad \text{(s)} \qquad [B2]$$

Substituting Eq. [B1] into Eq. [B2], we have

$$4.6\frac{(\beta - 1) \times 0.0029}{2 \times 10^{-9}} = 2{,}084{,}400 \quad \text{(s)} \qquad [B3]$$

from which $\beta$ is calculated to be 1.313.

Using Eq. [B1] and the calculated $\beta$ value, the work-hardening coefficient can be obtained as

$$H = \frac{\sigma}{\beta^2 \times 0.0029} = 18 \quad \text{(GPa)} \qquad [B4]$$

## ACKNOWLEDGMENTS

This work was conducted under National Research Council of Canada, Institute for Aerospace, Research Project No. JHM05. Constructive discussions with Dr. J.-P. Immarigeon are very much appreciated. Dr. T.G. Langdon is acknowledged for the useful review of the original manuscript.

## REFERENCES

1. B. Burton and G.L. Reynolds: *Phil. Mag.*, 1974, vol. 29, pp. 1359-70.
2. G.L. Reynolds, W.B. Beere, and B. Burton: *Met. Sci. J.*, 1977, vol. 11, pp. 213-18.
3. R. Raj and M.F. Ashby: *Metall. Trans.*, 1971, vol. 2, pp. 1113-27.
4. B. Burton: *Mater. Sci. Technol.*, 1989, vol. 5, pp. 1005-12.
5. R. Raj: *Metall. Trans. A*, 1975, vol. 5A, pp. 1499-1509.
6. B. Burton: *Diffusional Creep of Polycrystalline Materials*, Trans Tech Publications, Aedermannsdorf, Switzerland, 1977.
7. G. Malakondaiah, N. Prasad, G. Sundararajan, and P. Rama Rao: *Acta Metall.*, 1988, vol. 36, pp. 2167-81.
8. F. Garofalo: *Fundamentals of Creep and Creep-Rupture in Metals*, Macmillan Publishing Co., New York, NY, 1965.
9. B.F. Dyson and D. McLean: *Met. Sci. J.*, 1977, vol. 11, pp. 37-45.
10. A.K. Koul and R. Castillo: *Metall. Trans. A*, 1988, vol. 19A, pp. 2049-66.
11. R. Castillo, A.K. Koul, and J.-P.A. Immarigeon: in *Superalloys 1988*, S. Reichman, D.N. Duhl, G. Mauer, S. Antolovich, and C. Lund, eds., TMS-AIME, Warrendale, PA, 1988, pp. 805-13.
12. F.T. Furrillo, J.M. Davidson, J.K. Tien, and L.A. Jackman: *Mater. Sci. Eng.*, 1979, vol. 39, pp. 267-73.
13. A.K. Koul and R. Castillo: *ASM Materials Congress*, Pittsburgh, PA, Oct. 1993.
14. T.G. Langdon: *Phil. Mag.*, 1970, vol. 22, pp. 689-700.
15. R.C. Gifkins: *J. Australian Inst. Met.*, 1973, vol. 18, pp. 137-45.
16. F.W. Crossman and M.F. Ashby: *Acta Metall.*, 1975, vol. 23, pp. 425-40.
17. S.P. Temoshenko and J.N. Goodier: *Theory of Elasticity*, 3rd ed., McGraw-Hill, New York, NY, 1970.
18. E. Arzt, M.F. Ashby, and R.A. Verrall: *Acta Metall.*, 1983, vol. 31, pp. 1977-89.
19. R.W. Bailey: *J. Inst. Met.*, 1926, vol. 35, pp. 27-43.
20. E. Orowan: *J. West Scot. Iron-Steel Inst.*, 1946-47, vol. 54, pp. 45-96.
21. A. Seeger: in *Dislocations and Mechanical Properties of Crystals*, Wiley, New York, NY, 1957, pp. 243-329.
22. W.G. Johnston: *J. Appl. Phys.*, 1965, vol. 33, pp. 2716-30.
23. A.S. Krausz and H. Eyring: *Deformation Kinetics*, Wiley Interscience, New York, NY, 1975.
24. H. Frost and M.F. Ashby: *Deformation Mechanism Maps*, Pergamon Press, Elmsford, NY, 1982.
25. J. Rösler and E. Arzt: *Acta Metall.*, 1988, vol. 36, pp. 1043-51.
26. E. Arzt and J. Rösler: *Acta Metall.*, 1988, vol. 36, pp. 1053-60.
27. F.R.N. Nabaroo: *Theory of Crystal Dislocations*, Oxford University Press, London, 1967.
28. E. Orowan: *Proc. Phys. Soc.*, 1940, vol. 52, pp. 8-22.
29. R. Raj and M.F. Ashby: *Acta Metall.*, 1975, vol. 23, pp. 653-66.